Hartree–Fock calculations predict the correct order of magnitude for the spectrochemical strength, but the physical reason why $t_2^{m-1}e^{n+1}$ is higher than $t_2^m e^n$ has only an indirect relationship to the reason offered by ligand field theory. Hartree–Fock calculations corroborate the ligand field picture in associating a repulsion increase to the high-spin → low-spin transition, but the increase is predicted to be larger for the strong field complex—which contradicts the ligand field picture.

Apparently, ligand field theory (like atomic multiplet theory or Hund's rules) is better than the rationale upon which it has been built. The picture offered by Hartree–Fock calculations may be far from exact, but there are reasons to believe[27] that more reliable calculations (including electron correlation) will not affect the qualitative features of the model.

Registry No. CoF_6^{3+}, 15318-87-3; $Co(CN)_6^{3-}$, 14897-04-2.

Contribution from the Department of Chemistry,
North Dakota State University, Fargo, North Dakota 58105

Sharp Line Splittings in the Electronic Spectrum of Chloropentaamminechromium(III) Chloride

Kyu-Wang Lee and Patrick E. Hoggard*

Received September 1, 1987

A splitting of 16 cm^{-1} in the lowest energy spin-forbidden band has been observed in luminescence and excitation spectra of $[Cr(NH_3)_5Cl]Cl_2$. The two peaks have been assigned to the two components of the $^4A_{2g} \leftrightarrow {}^2E_g$ transition. Much larger ^2E_g splittings reported in the literature for this complex, and for the bromo and iodo analogues, have been reassigned to the splitting between the ^2E_g state and the lowest component of the $^2T_{1g}$ state. Ligand field calculations based on the exact ligand and counterion geometry yield a value of 1817 cm^{-1} for e_π of Cl^- and call into question earlier assumptions on the assignment of the spin-allowed transitions.

Introduction

Pentaammine complexes of chromium(III) and other metal ions have taken their places among the demonstration compounds of ligand field theory.[1-6] For d^3 and strong-field d^6 $[M(NH_3)_5X]^{n+}$ complexes the splitting of the first spin-allowed band is approximately equal to $(\Delta_N - \Delta_X)/4$, where Δ_N and Δ_X are the ligand field splitting parameters ($10Dq$) derived from the octahedral $[M(NH_3)_6]$ and $[MX_6]$ species.[1-7] Such correlations have been highly successful, as have those involving the second spin-allowed band of d^3 and d^6 complexes, although second-band splittings are less commonly observed experimentally.[8-10]

Splittings are also frequently observed among the three groups of sharp-line, spin-forbidden intraconfigurational transitions in d^3 complexes, $^4A_{2g} \rightarrow {}^2E_g$, $^2T_{1g}$, and $^2T_{2g}$ (in O_h notation). In particular, $^4A_{2g} \leftrightarrow {}^2E_g$ splittings have been reported for many Cr(III) complexes, because of the relative ease with which these lines can be detected in luminescence and absorption spectra. The pentaammine and tetraammine series were among the first to be investigated,[11-15] but the relatively large splittings observed (150–300 cm^{-1}) have long been a source of puzzlement. Ligand field theory, which works so well with the broad spin-allowed bands, appears to be incapable of generating splittings larger than 50 cm^{-1} for the pentaammines for any reasonable choice of parameters. Table I shows some representative literature values for the ^2E_g splitting in pentaammine complexes of Cr(III).

Table I. Reported ^2E_g Splittings for $[Cr(NH_3)_5X]^{n+}$ Complexes

X	splitting, cm^{-1}	anion	ref
Cl^-	170	ClO_4^-	14
	175	Cl^-	14
Br^-	225	Br^-	14
I^-	305	I^-	14
ONO^-	150	NO_3^-	14
	188	NO_3^-	13
H_2O	205	ClO_4^-	14
	87	NO_3^-	13
NCO^-	213	NO_3^-	16

The data for the halo pentaammines in Table I at least have some consistency. The ^2E_g splittings appear to increase with $\Delta_N - \Delta_X$. Ligand field theory predicts that the splitting of the first spin-allowed band depends on differences in $\Delta = 3e_\sigma - 4e_\pi$, where e_σ and e_π are the angular overlap model (AOM) destabilization parameters.[7] However, the splitting of the ^2E_g state has been shown to depend more on differences in $(e_\sigma + e_\pi)$ in AOM calculations.[17] Since Cl^-, Br^-, and I^- are stronger π-donors than NH_3 (which can be taken not to π-bond at all) and possibly weaker σ-donors, the sum $e_\sigma + e_\pi$ will be similar for NH_3 and the halides (except for F^-), even though $(3e_\sigma - 4e_\pi)$ values are quite different.

(1) Yamatera, H. *Bull. Chem. Soc. Jpn.* **1958**, *31*, 95.
(2) McClure, D. S. In *Advances in the Chemistry of the Coordination Compounds*; Kirschner, S., Ed.; Macmillan: New York, 1961; p 498.
(3) Wentworth, R. A. D.; Piper, T. S. *Inorg. Chem.* **1965**, *4*, 709.
(4) Wentworth, R. A. D.; Piper, T. S. *Inorg. Chem.* **1965**, *4*, 1524.
(5) Perumareddi, J. R. *J. Phys. Chem.* **1967**, *71*, 3155.
(6) Schläfer, H. L.; Gliemann, G. *Basic Principles of Ligands Field Theory*; Wiley-Interscience: London, 1969; Chapter 1.
(7) Schäffer, C. E.; Jørgensen, C. K. *Mat.-Fys. Medd.—K. Dan. Vidensk. Selsk.* **1965**, *34*(13).
(8) Glerup, J.; Mønsted, O.; Schäffer, C. E. *Inorg. Chem.* **1976**, *15*, 1399.
(9) Schläfer, H. L.; Martin, M.; Gausmann, H.; Schmidtke, H.-H. *Ber. Bunsen-Ges. Phys. Chem.* **1971**, *75*, 789.
(10) Decurtins, S.; Güdel, H. U.; Neuenschwander, K. *Inorg. Chem.* **1977**, *16*, 796.
(11) Porter, G. B.; Schläfer, H. L. *Ber. Bunsen-Ges. Phys. Chem.* **1967**, *68*, 316.
(12) Schläfer, H. L.; Martin, M.; Gausmann, H.; Schmidtke, H.-H. *Z. Phys. Chem.* (Munich) **1971**, *76*, 61.
(13) Shepard, W. N.; Forster, L. S. *Theor. Chim. Acta* **1971**, *21*, 135.
(14) Flint, C. D.; Matthews, A. P. *J. Chem. Soc., Faraday Trans. 2* **1973**, *69*, 419.
(15) Flint, C. D.; Matthews, A. P. *J. Chem. Soc., Faraday Trans. 2* **1977**, *73*, 655.
(16) Schönherr, T.; Schmidtke, H.-H. *Inorg. Chem.* **1979**, *18*, 2726.
(17) Hoggard, P. E. *Z. Naturforsch., A: Phys., Phys. Chem., Kosmophys.* **1981**, *36A*, 1276.

0020-1669/88/1327-0907$01.50/0

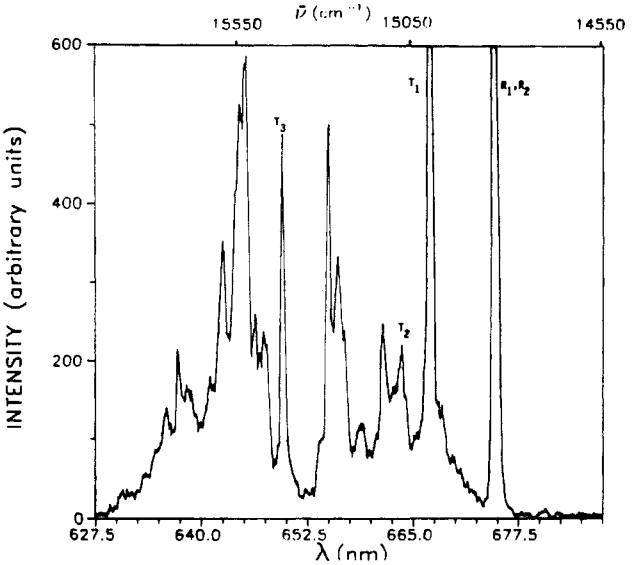

Figure 1. Uncorrected excitation spectrum of $[Cr(NH_3)_5Cl]Cl_2$ at 13 K. Luminescence is monitored at 685 nm, by using photon-counting detection.

Thus, the ^2E_g splittings predicted by ligand field theory for $[Cr(NH_3)_5X]^{2+}$ ($X = Cl^-, Br^-, I^-$) should be considerably smaller than the 50 cm^{-1} maximally achievable for the pentaammines in general.

Recently several factors that can significantly alter the doublet splittings have been incorporated into ligand field calculations. These include (1) using the exact ligand geometry to generate the ligand field potential rather than working within an assumed symmetry group,[18] (2) considering the field at the metal center generated by the nearest sphere of counterions,[19] (3) anisotropic π-bonding by ligands without cylindrical symmetry,[18] (4) misalignment of the ligand σ-bonding orbital with the ligand–metal axis,[20] and (5) phase coupling between coordinated atoms connected by a conjugated π-system.[21]

The last three factors can be disregarded for the halo pentaammines. A room-temperature crystal structure is known for $[Cr(NH_3)_5Cl]Cl_2$,[22] and it is thus possible to take into account the first two factors for this complex: the exact ligand geometry and the nearest sphere of chloride ions. We have therefore focused our attention on $[Cr(NH_3)_5Cl]Cl_2$. Although the crystal structure may be different at 13 K, at which temperature the excitation spectra reported here were measured, it can be expected that atom positions would change only by small translations in a new structure,[23] and thus transition energies would not change greatly.

In both the excitation and luminescence spectra of $[Cr(NH_3)_5Cl]Cl_2$ we have observed a small splitting of the lowest energy 0–0 line. In this paper we propose that this is the actual ^2E_g splitting, while the splittings shown in Table I for at least the chloro, bromo, and iodo pentaammine complexes are those between the ^2E_g state and the lowest component of the $^2T_{1g}$ state.

Experimental Section

$[Cr(NH_3)_5Cl]Cl_2$ was prepared by the method of Schlessinger.[24] It was recrystallized three times by slow evaporation in the dark.

Excitation spectra of $[Cr(NH_3)_5Cl]Cl_2$ were measured by monitoring the luminescence intensity of the vibronic sideband at 685 nm while scanning an EG&G PAR Dyescan laser through the range of DCM dye (Exciton Chemical Co.). The excitation wavelength was calibrated by using four neon optogalvanic resonance points. A microcrystalline sample was mounted with conductive grease on the cold head of an Air Products Displex CSA-202E cryostat. The emitted light was dispersed by a Spex Doublemate monochromator with 0.5-mm slits to a thermoelectrically cooled Hamamatsu R928 photomultiplier and detected with an EG&G PAR Model 1140A quantum photometer or an SRS boxcar integrator. Luminescence spectra were measured with the same apparatus, by exciting at 514 nm with Coumarin 500 dye and using 0.25-mm slits on the monochromator. Several different samples were studied, with consistent results.

Infrared spectra were recorded with a Mattson Cygnus 25 FT-IR spectrometer on a KBr pellet (mid-IR) and a Nujol mull on polyethylene film (far-IR). Visible–UV spectra were taken on IBM Model 9430 and Hewlett-Packard Model 8451A spectrophotometers.

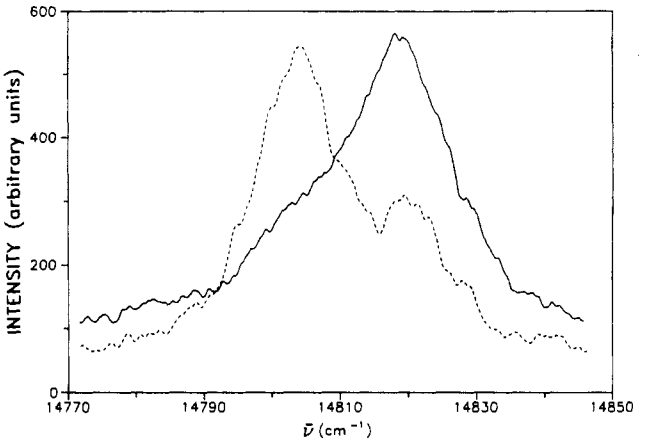

Figure 2. $^4A_{2g} \leftrightarrow {}^2E_g$ transitions in the 13 K excitation spectrum (solid line) and luminescence spectrum (dashed line) of $[Cr(NH_3)_5Cl]Cl_2$.

Table II. Assignment of Sharp-Line Positions in the Excitation Spectrum of $[Cr(NH_3)_5Cl]Cl_2$ at 13 K Measured from the Lowest Zero Phonon Peak (cm^{-1})

$\bar{\nu}$ − 14803	assignt	$\bar{\nu}$ − 14803	assignt
0 w	R_1	641 w	$T_1 + \nu$(CrN)
16 vs	R_2	653 vw	
187 vs	T_1	667 vw	
262 w	T_2	694 s	$R_2 + \delta(CrNH)_a$
312 w	$R_2 + \nu$(CrCl)	710 w	$T_2 + \nu$(CrN)
369 vw		759 m	$R_2 + \delta(CrNH)_b$
415 vw		795 vw	
434 vw		864 vw	$T_1 + \delta(CrNH)_a$
454 s	$R_2 + \nu$(CrN)	888 w	$T_3 + \nu$(CrCl)
593 s	T_3	923 vw	$T_1 + \delta(CrNH)_b$

Results and Discussion

Electronic Band Assignments. The excitation spectrum at 13 K of $[Cr(NH_3)_5Cl]Cl_2$ in the ^2E_g and $^2T_{1g}$ region is displayed in Figure 1. Expansion of the lowest energy peak reveals a shoulder on the low-energy side (Figure 2). The luminescence spectrum shows this splitting more distinctly, the low-energy peak being more intense and the higher energy peak appearing as a hot band. The separation of the main peak from the shoulder is 16 cm^{-1}. This is within the range of ligand field predictions for the ^2E_g splitting, and the room-temperature crystal structure shows there to be a single chromium site. We therefore assign the two peaks to the two ^2E_g components.

At 13 K the fraction of the population in a state 16 cm^{-1} above the ground state is 0.15. With this correction the absorption and emission spectra are not too dissimilar, and the two levels must be in good thermal contact. The luminescence lifetime (160 ns) was invariant with emission wavelength. At 30 K the relative intensities of the two ^2E_g lines in the excitation spectrum remained the same. In the luminescence spectrum the bandwidths at 30 K were too large to permit an estimation of the intensities.

The assignment of the three components of the $^4A_{2g} \rightarrow {}^2T_{1g}$ transition was made to those lines upon which the most consistent pattern of vibronic sidebands could be constructed in agreement with infrared results and with each other. Table II shows these

(18) Hoggard, P. E. *Coord. Chem. Rev.* **1986**, *70*, 85.
(19) Hoggard, P. E.; Lee, K.-W., submitted for publication in *Inorg. Chem.*
(20) Gerloch, M. *Magnetism and Ligand-Field Analysis*; Cambridge University Press: Cambridge, U.K., 1983.
(21) Ceulemans, A.; Dendooven, M.; Vanquickenborne, L. G. *Inorg. Chem.* **1985**, *24*, 1153.
(22) Hambley, T. W.; Lay, P. A. *Inorg. Chem.* **1986**, *25*, 4553.
(23) Figgis, B. N.; Reynolds, P. A.; Williams, G. A. *Acta Crystallogr., Sect. B: Struct. Crystallogr., Cryst. Chem.* **1981**, *B37*, 504.
(24) Schlessinger, G. *Inorganic Laboratory Preparations*; Chemical Publishing: New York, 1962; p 202.

Table III. Vibrational Frequencies from Room-Temperature Infrared and 13 K Luminescence and Excitation Spectra of $[Cr(NH_3)_5Cl]Cl_2$ (cm^{-1})

			vibronic intervals in excitation			
mode	IR	lumin	R_2	T_1	T_2	T_3
ν(CrCl)	307	301	296			295
ν(CrN)	432	484	448	454	448	
	459					
	471					
$\delta(CrNH)_a$	...	701	678	677		
$\delta(CrNH)_b$	775	770	743	736		

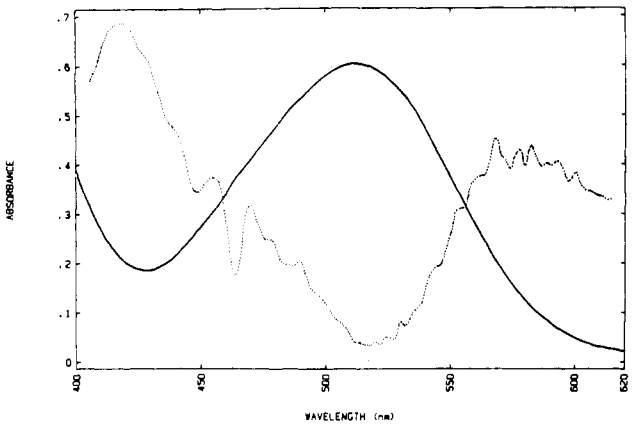

Figure 3. Second derivative (dotted line) of a portion of the room-temperature solution absorption spectrum (solid line) of $[Cr(NH_3)_5Cl]Cl_2$, showing the $^2T_{2g}$ structure beginning at 464 nm.

assignments together with assignments of several of the vibronic peaks. The vibronic structure associated with the luminescence spectrum[14] is mirrored in a similar pattern in the excitation spectrum based on the higher ^2E_g component (R_2). The R_2 line is the most intense in the spectrum, and consequently the vibronic structure stands out well. The T_1 line (which has heretofore been assigned to R_2),[14] representing the transition to the lowest $^2T_{1g}$ component, is also intense, and consequently most of the same vibronic pattern is evident, with little change in vibrational frequencies. The bands assigned to T_2 and T_3 are less intense, and only fragments of the expected patterns based on them are seen. The pattern for R_1 should be submerged within that for R_2.

This particular vibronic pattern consists for the most part of just four vibrational modes: ν(CrCl), ν(CrN), and two δ(CrNH) modes, which are derived from the IR-inactive τ_{2u} and IR-active τ_{1u} vibrations of the octahedral $[Cr(NH_3)_6]^{3+}$ parent.[25] The τ_{2u}-derived $\delta(CrNH)_a$ mode near 680 cm^{-1} is not present in the IR spectrum of $[Cr(NH_3)_5Cl]Cl_2$, even though the symmetry is broken. It is seen strongly in the luminescence spectrum, of both the chloropentaammine and the hexaammine.[14,26] Table III shows the variation in the frequencies of these four modes in IR and luminescence spectra and as vibronic intervals associated with four electronic origins in the excitation spectrum.

In the $^2T_{2g}$ region, expected near 450 nm, we were unable to observe sufficiently well-resolved sharp lines in the 13 K excitation spectrum of solid $[Cr(NH_3)_5Cl]Cl_2$. The second derivative of the room-temperature solution absorption spectrum, however, does show sharp line structure in this area, beginning with a large peak at 464 nm (21 550 cm^{-1}), as seen in Figure 3. We assign this line to the first component of the $^2T_{1g}$ group, but the spectrum is not resolved well enough to assign the other two components.

The transitions from the $^4A_{2g}$ state to the $^4T_{2g}$ and $^4T_{1g}$ excited states should, in spin-free C_{4v} symmetry, each be split into two components. Various investigators have noted a splitting of the first (lower energy) band[5,27,28] of around 2000 cm^{-1} in solution

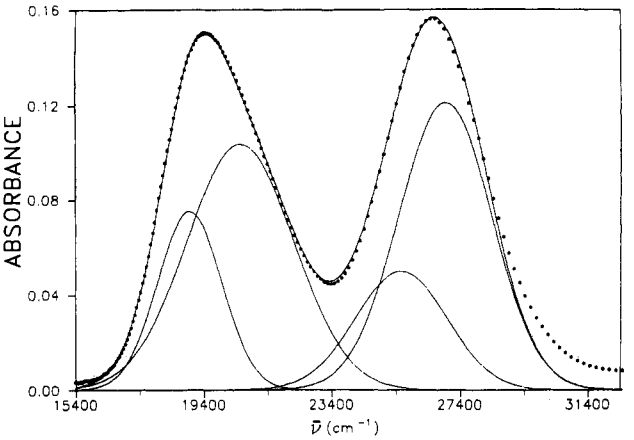

Figure 4. Best-fit resolution of the room-temperature solution absorption spectrum of $[Cr(NH_3)_5Cl]Cl_2$ into four Gaussian components. The fit was not extended past 29 000 cm^{-1} because of contributions from the tail of the charge-transfer band.

spectra, which has been used to assess the ligand field strength of the chloride ligand.[5,14,29] The second band shows no obvious splitting. The first band, in fact, also has a nearly symmetric profile, and it appears that the sharp but weak features from the $^2T_{2g}$ band(s) may have been mistaken for the quartet component expected in that area. In order to have some point of reference for the splittings of the two bands, we have fit the band profile to four component Gaussian curves. Figure 4 shows the results of this fit. We have used these peak positions as the experimental transition energies, although there is room for variation in the placement of the curves under the second band without substantial deterioration of the fit to the eye. In fact, using just one Gaussian curve instead of two yields a least-squares error only 4 times that of the best fit shown in Figure 4.

Ligand Field Calculations. Transition energies were obtained by diagonalization of the full 120 × 120 d^3 secular determinant, which was developed by means of a Hamiltonian including interelectronic repulsion (with a Trees correction[18]), spin–orbit coupling, and the ligand field potential. The ligand field potential matrix, $\langle d_i|V|d_j\rangle$, was generated by using the ligand positions from the room-temperature crystal structure,[22] as described previously.[18] In addition, the field from the eight nearest chloride counterions, which form a distorted cube around the $[Cr(NH_3)_5Cl]^{2+}$ complex, was included in the ligand field potential by means of the AOM parameter, $e_{\sigma A}$. Previous work[19] would cause us to expect a value for $e_{\sigma A}$ around 200 cm^{-1}.

The adjustable parameters used in the model were the AOM parameters $e_{\sigma N}$, $e_{\sigma Cl}$, $e_{\pi Cl}$, and $e_{\sigma A}$, Racah parameters B and C, the Trees correction parameter α, and the spin–orbit coupling parameter ζ. The AOM parameters were constrained to vary with the distance of the donor atom from the metal, $e_{\sigma N}$ as R^{-5} (which did not prove to be significant) and $e_{\sigma A}$ as R^{-3}.[19]

The assignment of the energy eigenvalues to the proper states was done by classifying the associated eigenfunctions as quartets or doublets. The three-electron atomic basis functions were divided into three groups: spin $\pm^3/_2$ functions, spin $\pm^1/_2$ functions of the type (a^+,b^+,c^-), and spin $\pm^1/_2$ functions of the type (a^+,a^-,b^+). With no spin–orbit coupling, the first group can occur only in quartet eigenfunctions, and the third group only in doublet eigenfunctions. A comparison of the sums of the coefficients in the three groups was used to assign the spin parentage of each eigenfunction. This procedure proved satisfactory even when doublet and quartet regions overlapped. Further assignments to O_h or C_{4v} labels were made by performing an approximate calculation in the D_4^* basis.[17]

The experimental transition energies used in the fitting process are given in Table IV. By variance of the eight parameters in

(25) Loehr, T. M.; Zinich, J.; Long, T. V. *Chem. Phys. Lett.* **1970**, *7*, 183.
(26) Flint, C. D.; Greenough, P. *J. Chem. Soc., Faraday Trans. 2* **1972**, *68*, 897.
(27) Linhard, M.; Weigel, M. *Z. Anorg. Allg. Chem.* **1951**, *266*, 49.
(28) Linhard, M.; Weigel, M. *Z. Phys. Chem. (Munich)* **1955**, *5*, 20.
(29) Perumareddi, J. R. *Coord. Chem. Rev.* **1969**, *4*, 73.

Table IV. Calculated and Experimental Transition Energies for $[Cr(NH_3)_5Cl]Cl_2$ (cm^{-1}; Data at 13 K Unless Otherwise Noted)

state (O_h)	exptl	calcd[a]	calcd[b]
^2E_g	14803	14795	14792
	14819	14811	14803
$^2T_{1g}$	14990	14991	15003
	15065	15067	15056
	15396	15407	15414
$^2T_{2g}$	21550[c]	21561[d]	21588
$^4T_{2g}$	18950[c]	19062[e]	19147
	20530[c]	20692[f]	20607
$^4T_{1g}$	25550[c]	25332[g]	25241
	26910[c]	26868[h]	26905

[a] Best fit with actual ligand geometry and counterion field: $e_{\sigma N}$ = 7149 ± 180, $e_{\sigma Cl}$ = 7190 ± 109, $e_{\pi Cl}$ = 1817 ± 113, $e_{\sigma A}$ = 244 ± 173, B = 714 ± 7, C = 2757 ± 17, α (Trees parameter) = 186 ± 10, ζ = 1 ± 16000. [b] Best fit in D_4^* basis: $e_{\sigma N}$ = 6870, $e_{\sigma Cl}$ = 7127, $e_{\pi Cl}$ = 1664, B = 728, C = 2656, α = 221, ζ = 103. [c] Room-temperature data. [d] Other two components at 21779, 21831. [e] 18981, 18981, 19144, 19144. [f] 20692, 20692. [g] 25275, 25275, 25390, 25390. [h] 26868, 26868.

the model just described, these energies were fit, with use of the Powell parallel subspace optimization procedure.[30,31] The function minimized was

$$f = \sum Q^2 + 10D_{T2}^2 + 100\sum D^2 + 1000S^2 \qquad (1)$$

where Q, D_{T2}, D, and S represent the differences between the experimental and calculated quartet energies, the average $^2T_{2g}$ energy, the ^2E_g and $^2T_{1g}$ energies, and the ^2E_g splitting, respectively. The weighting factors in this function are in approximate proportion to the inverse square of the corresponding experimental uncertainties. The experimental data were acquired at two different temperatures and are thus not entirely self-consistent. However, the function in eq 1 does weight the 13 K data much more heavily.

The doublet energies represent transitions to single states (actually to degenerate pairs of Kramers doublets) and can be matched one-to-one with calculated transition energies. The $^4A_{2g} \rightarrow {}^4T_{2g}$ and $^4A_{2g} \rightarrow {}^4T_{1g}$ transitions each consist of six distinct components. In calculations, each set of six can be divided, in approximate accordance with the spin-free C_{4v} approximation, into closely spaced groups of two and four components. The average transition energies within these groups were used to match the band maxima from Gaussian resolution of the experimental absorption spectrum. The best-fit calculated energies and the corresponding parameter set appear in Table IV. The uncertainties reported for the best-fit parameters are those resulting only from the error propagated from average experimental uncertainties of 100 cm^{-1} for the quartets, 10 cm^{-1} for the ^2E_g and $^2T_{1g}$ lines, 20 cm^{-1} for the $^2T_{2g}$ peak, and 1 cm^{-1} for the ^2E_g splitting.[32] Actual error limits, which would recognize sizable tolerances in the calculated transition energies, would be larger. Although constraints were set up for each of them, all parameters fell well within their prescribed limits, except for ζ, for which a penalty function was invoked near its lower limit of 0.

The value of ζ can in any case be seen to be virtually without significance because of the large error margin associated with it. It can be argued that the other parameters are all reasonable. The value of 244 cm^{-1} for $e_{\sigma A}$, the d-orbital destabilization caused by the nearest anions, can be compared with values of 201 or 319 cm^{-1} for the potassium ions in $K_3[Cr(CN)_6]$ (depending on which crystal structure obtained at the measurement temperatures).[19] The 244-cm^{-1} value applies only to the closest Cl^-, 4.25 Å distant. The farthest of the group, 4.41 Å from the Cr, would have $e_{\sigma A}$ = 218 cm^{-1}, because of the falloff as R^{-3}. The 186-cm^{-1} value for the Trees parameter α may appear to be too large, in comparison with the 70 cm^{-1} used for atomic spectra, but for six-coordinate complexes of Cr(III) in which a Trees correction was employed and data from the $^2T_{2g}$ bands were included, α has consistently been found to be larger than the free-ion value: 218 cm^{-1} for $K_3[Cr(NCS)_6]$[18] and 203 or 212 cm^{-1} for $K_3[Cr(CN)_6]$.[19]

Perhaps the greatest surprise is the large value for $e_{\pi Cl}$, approximately twice as large as currently accepted values.[33-37] Lever has noted that the result obtained depends on the assignment of the components of the second spin-allowed band.[35] In the spin-free C_{4v} approximation this band is split into ^4E and $^4A_2$ components. From the diagonal transition energies (upon which most AOM parameters now in use are based), the ^4E component will lie higher if the quantity $3e_\sigma + 4e_\pi$ is larger for NH_3 than for Cl^-, or whatever the sixth ligand happens to be. and lower otherwise.[7] An analysis of single-crystal polarized absorption spectra of *trans*-$[Cr(en)_2Cl_2]ClO_4$ led Dubicki and Day to assign the higher energy component to ^4E for this compound,[36] an assignment that would carry over to the chloro pentaammine complex as well. In Lever's analysis of the spectrum of $[Cr(en)_2Cl_2]^+$, the value of $e_{\pi Cl}$ would change from 900 to 1570 cm^{-1} if the assignment were reversed.[35]

In our analysis, the large value of e_π is required because of the splitting within the $^2T_{1g}$ band, which depends directly on $e_{\pi Cl} - e_{\pi N}$.[8,38] This in turn causes ^4E to fall below $^4A_2$ in calculations. In reexamining Dubicki and Day's spectra, we are led to suggest that the band they assigned as the $^4A_2$ component of the $^4T_{1g}$ band is actually $^2T_{1g}(O_h)$ and a shoulder on the high-energy side of the main ^4E band should be assigned to $^4A_2$.

A large $e_{\pi Cl}$ value requires that the value of $e_{\sigma Cl}$ also be large, in order to maintain the ligand field splitting parameter Δ_{Cl} ($=3e_{\sigma Cl} - 4e_{\pi Cl}$) at a value determined in large part by the splitting of the first spin-allowed band. With use of the best-fit parameters, Δ_{Cl} is 14300 cm^{-1}.

The experimental transition energies may also be fit in the D_4^* approximate symmetry group.[17] The best-fit energies are included in Table IV. The error function (eq 1) is 2.5 times larger for these results. Using the actual ligand positions, while the anion field was ignored ($e_{\sigma A}$ = 0), improved the best-fit error function to 1.2 times that of the best fit with the anion field (and an adjustable $e_{\sigma A}$ value). The anion geometry is close enough to cubic that it contributes little to the splitting of the t_{2g} orbitals. But when the anion field is included, it raises the energies of the t_{2g} orbitals uniformly, causing the ligand AOM parameters to appear higher than they would if the anion field were neglected. Thus, for comparison with AOM parameters calculated in the absence of the counterion field (as is appropriate for solution data), the best-fit values with no anion field are more appropriate: $e_{\sigma N}$ = 6888, $e_{\sigma Cl}$ = 7027, $e_{\pi Cl}$ = 1669 cm^{-1}. Since our data were from a mix of solid-state and solution spectra, we were unable to explore the question of the extent to which differences between them might be explained by the anion field.

Zero Phonon Line Intensities. The assignment of the small shoulder under the envelope of the R_2 peak to R_1 does raise the question of why the intensity of one zero phonon line should be much smaller than that of the other. Ruby provides a prominent example of a system in which the R_1 and R_2 lines have similar heights, and there are enough examples where this is approximately so that some may be tempted to induce from this a general rule.

Spin-forbidden lines acquire intensity by borrowing from spin-allowed transitions through spin–orbit coupling.[39] The spin-allowed d–d transitions in turn, since they are Laporte-forbidden, must themselves borrow intensity from allowed transitions. One approach to estimating the relative intensities of d^3 spin-forbidden transitions is to compare the eigenfunctions of the excited doublet states, with and without spin–orbit coupling, in order to

(30) Powell, M. J. D. *Comput. J.* **1964**, *7*, 155.
(31) Kuester, J. L.; Mize, J. H. *Optimization Techniques with Fortran*; McGraw-Hill: New York, 1973.
(32) Clifford, A. A. *Multivariate Error Analysis*; Wiley-Halstad: New York, 1962.
(33) Lever, A. B. P. *Coord. Chem. Rev.* **1968**, *3*, 119.
(34) Fee, W. W.; Harrowfield, J. N. M. *Aust. J. Chem.* **1969**, *23*, 1049.
(35) Keeton, M.; Chou, B. F.; Lever, A. B. P. *Can. J. Chem.* **1971**, *49*, 192.
(36) Dubicki, L.; Day, P. *Inorg. Chem.* **1971**, *10*, 2043.
(37) Barton, T. J.; Slade, R. C. *J. Chem. Soc., Dalton Trans.* **1975**, 650.
(38) Forster, L. S.; Rund, J. V.; Fucaloro, A. F. *Inorg. Chem.* **1984**, *88*, 5012.
(39) Sugano, S. *Suppl. Prog. Theor. Phys.* **1960**, *No. 14*, 66.

Table V. Calculated Intensities for the Eight Intraconfigurational Spin-Forbidden Transitions in $[Cr(NH_3)_5Cl]Cl_2$ (Relative to $Int(R_2) = 1.0$; $R = \langle Q_i|er|Q_i\rangle / \langle Q_i|er|Q_j\rangle$)

transition		$\zeta = 1$,[a] $R = 1$	$\zeta = 1$,[a] $R = 25$	$\zeta = 100$,[b] $R = 1$	$\zeta = 100$,[b] $R = 25$
^2E_g	R_1	0.40	0.39	1.91	1.87
	R_2	1.00	1.00	1.00	1.00
$^2T_{1g}$	T_1	0.06	0.62	0.65	0.85
	T_2	0.19	0.79	0.43	1.23
	T_3	0.56	0.55	0.43	0.44
$^2T_{2g}$	B_1	2.33	12.75	1.75	7.02
	B_2	1.92	5.50	0.87	2.54
	B_3	4.47	8.93	3.69	6.99

[a] Best-fit parameters of Table IV. [b] $e_{\sigma N} = 7092$, $e_{\sigma Cl} = 7156$, $e_{\pi Cl} = 1784$, $e_{\sigma A} = 190$, $B = 712$, $C = 2763$, $\alpha = 186$ (best fit with $\zeta = 100$).

estimate the amount of (unperturbed) quartet character. This approach, though it neglects all vibronic contributions to the scrambling of states,[40] allows us to consider the pure electronic mixing more thoroughly than is normally done, in effect by including all excited states at all orders of perturbation.

To estimate the transition moment between a quartet state, $|Q_i\rangle$, and a doublet state, $|D_j\rangle$, we express the quartet eigenfunction in terms of an admixture of small amounts of doublet character through interaction with all 80 doublet states:

$$|Q'_i\rangle = |Q_i\rangle + a_{ji}|D_j\rangle + \sum_{k\neq j}^{80} a_{ki}|D_k\rangle \quad (2)$$

The unprimed labels refer to the eigenfunctions in the absence of spin–orbit coupling. Likewise the doublet will be mixed with small amounts of each of the 40 quartet states:

$$|D'_j\rangle = |D_j\rangle + b_{ij}|Q_i\rangle + \sum_{k\neq i}^{40} b_{kj}|Q_k\rangle \quad (3)$$

The coefficients

$$a_{ij} = \langle D_i|Q'_j\rangle \qquad b_{ij} = \langle Q_i|D'_j\rangle$$

are dot products of the unperturbed with the perturbed eigenfunctions. These can be calculated straightforwardly after performing diagonalizations with and without spin–orbit coupling.

The transition moment between states $|Q'_i\rangle$ and $|D'_j\rangle$ is then

$$Q_{ij} = \langle Q'_i|er|D'_j\rangle = b_{ij}\langle Q_i|er|Q_i\rangle + a_{ji}\langle D_j|er|D_j\rangle + \sum_{k\neq j}^{80}\alpha_{ki}\langle D_k|er|D_j\rangle + \sum_{k\neq i}^{40} b_{kj}\langle Q_i|er|Q_k\rangle \quad (4)$$

The terms in the summations are transition moments for spin-allowed but Laporte-forbidden transitions. For purposes of this calculation we will assume that they are all equal. The first two terms represent permanent dipole moments for what in this case will be the ground and excited states. The states of interest are all derived from the t_{2g}^3 configuration, so we may assume that the two permanent dipole terms are equal. The permanent dipole and the transition dipoles are likely to be quite different for most molecules, however. $[Cr(NH_3)_5Cl]^{2+}$ should have a moderate permanent dipole, while the Laporte-forbidden transition dipoles can be expected to be smaller.

Table V shows the results of this calculation for the eight t_{2g}^3 intraconfigurational transitions at two different ratios of the permanent dipole moment to the transition moment, using the best-fit parameters of Table IV. Each intensity value was arrived at by summing the eight contributions from the four $^4A_{2g}$ components to the two doublet components. The calculated relative intensities are sensitive to the ratio of permanent to transition dipole moments. They are also sensitive to the ligand field parameters. Table V also lists calculated relative intensities for a best-fit set of parameters with ζ fixed at 100 cm^{-1}.

The approximation is too crude and the results are too sensitive to the parameters used to make any claim that the R_1 band is predicted to be much less intense than R_2. However, at least in near-tetragonal symmetry it does appear that large variations in the R_1/R_2 intensity ratio can be expected over a range of complexes. Also, since the relative intensities of the ^2E_g, $^2T_{1g}$, and $^2T_{2g}$ groups seem to depend heavily on R, the ratio of the permanent to the average transition dipole moment, and less heavily on the parameter set, it may be possible to estimate R from the doublet extinction coefficients. A ratio of about 25 is suggested by our data.

Conclusions. The splittings shown in Table I, which were formerly assigned to the R_1–R_2 splitting of the ^2E_g states, have been reassigned to the R_2–T_1 splitting for $[Cr(NH_3)_5Cl]Cl_2$, and this should apply as well to the bromo and iodo pentaammines. This suggestion was put forward by Güdel on an earlier occasion.[10] Chemically this makes much more sense. In the old interpretation, the order of increasing splitting among the halo pentaammines, Cl < Br < I, had to be explained, if at all, in terms of differences in ligand field strength, although ligand field calculations show very little dependence of the doublet transition energies on Δ.[17] The R_2–T_1 splitting, on the other hand, depends inversely on the total $^2T_{1g}$ splitting, which in turn depends most on differences in e_π.[8,38] Given the expected order of π-donor strengths, Cl > Br > I, the total $^2T_{1g}$ splitting should be greatest for the chloro pentaammine complex and the R_2–T_1 splitting correspondingly smallest.

Acknowledgment. This material is based upon work supported in part by the National Science Foundation under Grant RII8610675. We also thank the donors of the Petroleum Research Fund, administered by the American Chemical Society, for their support of this research.

Registry No. $[Cr(NH_3)_5Cl]Cl_2$, 13820-89-8.

(40) Ballhausen, C. J.; Bak, T. A. *J. Mol. Struct.* **1980**, *59*, 265.